Science of the Total Environment 925 (2024) 171585

Contents lists available at ScienceDirect

Science of the Total Environment

journal homepage: www.elsevier.com/locate/scitotenv

Sensitivities of ozone to its precursors during heavy ozone pollution events in the Yangtze River Delta using the adjoint method

Yu-Hao Mao [a,b,*], Yongjie Shang [a], Hong Liao [a,b], Hansen Cao [c], Zhen Qu [c], Daven K. Henze [c]

[a] Jiangsu Key Laboratory of Atmospheric Environment Monitoring and Pollution Control/Jiangsu Collaborative Innovation Center of Atmospheric Environment and Equipment Technology, School of Environmental Science and Engineering, Nanjing University of Information Science and Technology (NUIST), Nanjing 210044, China
[b] Key Laboratory of Meteorological Disaster, Ministry of Education(KLME)/Collaborative Innovation Center on Forecast and Evaluation of Meteorological Disasters (CIC-FEMD)/International Joint Research Laboratory on Climate and Environment Change (ILCEC), NUIST, Nanjing 210044, China
[c] Department of Mechanical Engineering, University of Colorado, Boulder, CO 80309, USA

HIGHLIGHTS

- Four types of synoptic weather patterns are classified during heavy ozone pollution events.
- Industry and transportation emissions from the YRD have a high impact on ozone in Nanjing
- 10 % reduction of anthropogenic NO_x and NMVOCs emissions in the YRD reduces the ozone in Nanjing by 3.40 and 0.96 μg m^{-3}.

GRAPHICAL ABSTRACT

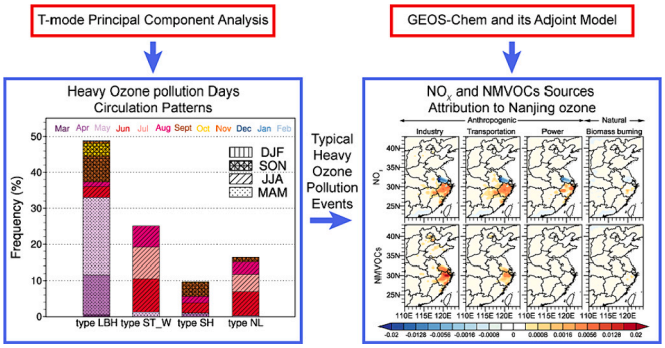

ARTICLE INFO

Editor: Jianmin Chen

Keywords:
Heavy ozone pollution
Precursor emissions
Source attribution
Adjoint method
Circulation patterns

ABSTRACT

Although the concentrations of five basic ambient air pollutants in the Yangtze River Delta (YRD) have been reduced since the implementation of the "Air Pollution Prevention and Control Action Plan" in 2013, the ozone concentrations still increase. In order to explore the causes of ozone pollution in YRD, we use the GEOS–Chem and its adjoint model to study the sensitivities of ozone to its precursor emissions from different source regions and emission sectors during heavy ozone pollution events under typical circulation patterns. The Multi-resolution Emission Inventory for China (MEIC) of Tsinghua University and 0.25° × 0.3125° nested grids are adopted in the model. By using the T–mode principal component analysis (T–PCA), the circulation patterns of heavy ozone pollution days (observed MDA8 O_3 concentrations ≥160 μg m^{-3}) in Nanjing located in the center area of YRD from 2013 to 2019 are divided into four types, with the main features of Siberian Low, Lake Balkhash High, Northeast China Low, Yellow Sea High, and southeast wind at the surface. The adjoint results show that the contributions of emissions emitted from Jiangsu and Zhejiang are the largest to heavy ozone pollution in Nanjing. The 10 % reduction of anthropogenic NO_x and NMVOCs emissions in Jiangsu, Zhejiang and Shanghai

* Corresponding author at: Jiangsu Key Laboratory of Atmospheric Environment Monitoring and Pollution Control/Jiangsu Collaborative Innovation Center of Atmospheric Environment and Equipment Technology, School of Environmental Science and Engineering, Nanjing University of Information Science and Technology (NUIST), Nanjing 210044, China.
E-mail address: yhmao@nuist.edu.cn (Y.-H. Mao).

https://doi.org/10.1016/j.scitotenv.2024.171585
Received 7 October 2023; Received in revised form 6 March 2024; Accepted 6 March 2024
Available online 9 March 2024

could reduce the ozone concentrations in Nanjing by up to 3.40 μg m^{-3} and 0.96 μg m^{-3}, respectively. However, the reduction of local NMVOCs emissions has little effect on ozone concentrations in Nanjing, and the reduction of local NO_x emissions would even increase ozone pollution. For different emissions sectors, industry emissions account for 31 %–74 % of ozone pollution in Nanjing, followed by transportation emissions (18 %–49 %). This study could provide the scientific basis for forecasting ozone pollution events and formulating accurate strategies of emission reduction.

1. Introduction

High concentrations of surface ozone pollution are harmful to human health and crop growth (Feng et al., 2022; Liu et al., 2022a) and have a huge impact on climate change (Wang et al., 2022b). The concentrations of six basic ambient air pollutants except ozone have significantly reduced after 2013 when China has implemented more stringent control measures on air pollutant emissions (Fu et al., 2019). However, the report on the State of the Ecology and Environment in China (MEE, 2013, 2019) shows that the annual ozone assessment concentrations (90th percentile of the annual maximum daily 8–hour average ozone) have increased from 144 μg m^{-3} to 179 μg m^{-3} in the Yangtze River Delta (YRD) from 2013 to 2019. Nanjing is a key developing city in the center area of the YRD and the ozone pollution in Nanjing has maintained a consistent growth trend with the YRD. The number of days with maximum daily 8–hour average ozone (MDA8 O_3) concentrations in Nanjing exceeding the national air quality standard of 160 μg m^{-3} increased from 50 days in 2015 to 69 days in 2019 (NMEEB, 2016, 2019). Therefore, the prevention and control of the increasingly serious ozone pollution is currently an important issue in the YRD.

Non-methane volatile organic compounds (NMVOCs) and nitrogen oxides (NO_x) have a highly nonlinear relationship to the formation of ozone. The ozone pollution is effectively controlled only by accurately analyzing the sensitivities of ozone formation to its precursor emissions (Chen et al., 2021; Gao et al., 2017; Liu et al., 2021; Mao et al., 2022b; Wang et al., 2022a; Zhang et al., 2021). The observation-based analysis of Chen et al. (2021) indicated that the surface ozone concentrations in the YRD averagely increased by 8 ppbv from 2014 to 2019 due to the decrease of NO_2 by about 4 ppbv. The GEOS–Chem simulations indicated the anthropogenic NMVOCs/NO_x emission reduction ratios of 1:1 in the YRD in May, July and September, and 2:1 in October 2017 could reduce the surface ozone concentrations in Nanjing (Mao et al., 2022b). Satellite retrievals suggested that the urban areas of Nanjing were generally under a NMVOCs–limited regime in 2016–2019; in contrast, the suburban regions were mostly NO_x–limited areas and NMVOCs–NO_x–limited areas (Wang et al., 2021a).

The key of ozone pollution control is to identify the important source regions and emission sectors (Ge et al., 2021; Lei et al., 2022; Liu et al., 2020b). During the G20 Summit in September 2016, the results of WRF–Chem and backward trajectory suggested that the polluted air mass that affected the ozone concentrations in the lower-level troposphere in Hangzhou mainly came from Zhejiang and Jiangsu province (Wang et al., 2021c). Gong et al. (2018) combined statistical and backward trajectory models to find that the difference between the contributions of the terrestrial and marine airflow to surface MDA8 O_3 in Shanghai in 2014–2016 was 31–56 μg m^{-3}. Wang et al. (2019c) applied the CMAQ adjoint model to show that the contribution of ozone and its precursors from Anhui, Hubei and Jiangsu to the surface ozone in the YRD region was 69 % in June 2010. For different emission sectors, Fang et al. (2021) used multi-modeling approaches to find that transportation and industry sectors contributed to surface ozone pollution over the Pearl River Delta in 2017 by 29.2 %–31.5 % and 11.4 %–13.0 %, respectively. For Zhengzhou from May to September 2017, the results of positive matrix factorization showed that the main NMVOCs emission sources were vehicle exhaust, coal and biomass burning and solvent usage in the NMVOCs–limited areas (Li et al., 2019b).

Atmospheric chemistry model is a useful tool to analyze the source of ozone pollution or the sensitivities of ozone to its precursor emissions. Currently, the commonly used methods include backward trajectory method (Li et al., 2019b; Xu et al., 2018), tagged tracer method (Li et al., 2019a; Liu et al., 2019b; Wang et al., 2019a), emission perturbation sensitivity simulation (Liu and Wang, 2020b; Wang et al., 2010), and adjoint model (Jiang et al., 2015; Wang et al., 2019c; Zhang et al., 2009). The backward trajectory models only quantify the potential contribution of regional transport to receptor area, and could not identify the emission sectors; the tagged tracer method only obtains the total contribution of specific emissions and tracers in the designated areas to pollution, and could not distinguish the contribution on the model grid scale; and the model sensitivity method needs to conduct multi-group model simulations by perturbing the emissions of ozone precursors with different ratios, which is limited to the number of simulations. In contrast, the adjoint model can efficiently calculate the sensitivities of pollutant to its precursor emissions on the model grid scale during a single simulation (Henze et al., 2007, 2009; Wang et al., 2019c). Previous studies have shown that the GEOS–Chem and its adjoint model can efficiently simulate the sensitivities of ozone to its precursor emissions from different source regions and emission sectors (Qu et al., 2020; Wang et al., 2021b; Wang et al., 2020).

The meteorological fields are also important factors to the formation of ozone pollution. Liu et al. (2019a) showed that meteorological factors can explain 43 %–64 % of daily surface ozone changes in North China from April to October 2013–2017 by using a method of reconstruction of ozone concentrations based on weather types. The appearance of meteorological factors generally corresponds to the large–scale circulation systems. The subtropical high and typhoon system often appear in the YRD and Pearl River Delta (Huang et al., 2006; Hung and Lo, 2015; Shu et al., 2016) and are favorable to the occurrence of heavy ozone pollution. Under the control of subtropical high, sunny weather with high temperature, low cloud cover and low humidity are conducive to photochemical reactions. In the regions controlled by the peripheral subsidence airflows of typhoon, high temperature and strong vertical transport also cause the increase of ozone concentrations (Hung and Lo, 2015; Shu et al., 2016).

Numerous studies have shown that the principal component analysis method is stable and accurate to classify large–scale weather circulation (Liu et al., 2018; Miao et al., 2019). In this study, the T–mode principal component analysis (T–PCA) is used to classify the typical circulation patterns during heavy ozone pollution episodes from April 2013 to December 2019 in Nanjing. The classification of circulation patterns is helpful to predict the heavy ozone pollution events. Then the GEOS–Chem and its adjoint model are used to analyze the sensitivities of ozone to its precursor emissions from different source regions and emission sectors during heavy ozone pollution under the typical circulation patterns in Nanjing, which can provide a scientific basis for accurate emission control of precursors of ozone under the typical circulation conditions. Section 2 presents the data and methods, including the descriptions of the GEOS–Chem forward model and its adjoint, observations and the T–PCA method. Section 3.1 shows the evaluations of the GEOS–Chem model performance. Section 3.2 presents the typical synoptic patterns during heavy ozone pollution. Section 3.3 comprises the sensitivities of ozone to its precursor emissions during typical heavy ozone pollution events in Nanjing. Finally, Section 4 shows main conclusions of this research.

2. Methods

2.1. GEOS–Chem forward model and its adjoint

The GEOS–Chem chemical transport model and its adjoint model (v35k, http://wiki.seas.harvard.edu/geos-chem/index.php/GEOS-Chem_Adjoint_v35) are applied to investigate the heavy ozone pollution in the YRD. The model is driven by the GEOS–FP assimilated meteorological data provided by the Goddard Earth Observing System (GEOS) of the Earth Modelling and Assimilation Office (GMAO) and with a temporal resolution of 1 h for surface variables and boundary layer height and 3 h for others. The model adopts a tropospheric "NO_x–O_x–HC–aerosol" chemical mechanism (Bey et al., 2001; Mao et al., 2013; Park et al., 2004; Wang et al., 1998) to simulation ozone pollution. We use a nested model with a horizontal resolution of 0.25° × 0.3125° in the East Asian region (70°–140°E, 15°–55°N), and the boundary conditions are provided by a global model with a horizontal resolution of 2° × 2.5°.

The Emissions Database for Global Atmospheric Research (EDGAR v4.2, http://wiki.seas.harvard.edu/geos-chem/index.php/EDGAR_v4.2_anthropogenic_emissions) is used for global anthropogenic emissions. The anthropogenic emissions in China for 2017 are from the Multi–resolution Emission Inventory for China (MEIC, Zheng et al., 2018). The MEIC emission inventory includes the emissions of ozone precursors, such as nitrogen oxides (NO_x), carbon monoxide (CO) and NMVOCs, from four emission sectors (industry, transportation, residential and power sectors) and with a temporal resolution of one month. Fig. S1 shows the monthly mean emissions of ozone precursors in the MEIC emission inventory from May to July 2017. For spatial distributions of emissions, the anthropogenic NO_x emissions are mainly concentrated in the Beijing–Tianjin–Hebei and the YRD region, with the highest NO_x emissions in the YRD region (~11 Gg mon^{-1}). Industry sector accounts for about 42 % of anthropogenic NO_x emissions in central and eastern China (97°–125°E, 18°–45°N), followed by transportation sector (37 %), power sector (19 %), and residential sector (3 %). The anthropogenic CO emissions are mainly concentrated in the central and eastern regions of China and the Sichuan Basin. The significant high values of CO emissions are above 70 Gg mon^{-1} in the Beijing–Tianjin–Hebei, YRD, and Pearl River Delta regions. The contributions of CO emissions in central and eastern China from industry sector, residential sector, and transportation sector are about 43 %, 33 %, and 21 %, respectively, while those from power sector are <4 %. Similar to CO emissions, the anthropogenic NMVOCs emissions are also concentrated in the central and eastern regions of China and the Sichuan Basin. The anthropogenic NMVOCs emissions are highest in the YRD with the emission of about 14 GgC mon^{-1}. For the anthropogenic NMVOCs emissions, industry sector contributes about 68 % in central and eastern China, follow by transportation sector (20 %), residential sector (12 %), and power sector (<1 %).

For natural emissions, soil NO_x emissions are calculated by algorithm of Hudman et al. (2010, 2012). Lightning NO_x emissions are calculated using the parameterization methods (Murray et al., 2012) of Price and Rind (1992) and Ott et al. (2010). Biogenic NMVOCs emissions are from Model of Emissions of Gases and Aerosols from Nature (MEGAN v2.1, Guenther et al., 2012). The fourth–generation global fire emissions database (Werf et al., 2017) is implemented for calculating biomass burning emissions with a temporal resolution of one month.

In addition, the GEOS–Chem adjoint model simulates the ozone concentrations at the central height of the first layer grid (about 75 m above the ground), which may not be appropriate to compare with the observed surface ozone concentrations. In the present study, we adopt the method by Lapina et al. (2015) and Travis and Jacob (2019) to make fair comparisons between model simulations and observations, which applied ozone deposition velocity and aerodynamic resistance to correct the simulated ozone concentrations in the forward simulation from the central height of the model first layer grid to 2 m above the surface.

2.2. Observations

The hourly observations of ozone in central and eastern China during April 2013 to December 2019 are downloaded from the China National Environmental Monitoring Centre (http://www.cnemc.cn/zzjj/jcwl/dqjcwl/201711/t20171108_645109.shtml). For each city, all stations in the monitoring network are selected and the observations are averaged over these stations to represent the ozone concentrations in the city. The ozone concentrations reported at the monitoring sites are in micrograms per cubic meter (μg m^{-3}), and under the standard state (273 K, 101.325 kPa) before September 1, 2018 and then under the reference state (298.15 K, 1013.25 hPa). The ozone concentrations are uniformly converted to standard state in the study. The MDA8 O_3 concentrations are calculated to evaluate ozone pollution in the YRD. To ensure the validity of the observation data, the 8–hour averages are calculated when at least 6 h of observations are available and the number of valid 8–hour average values is >14 in a day. If the 14 valid values are not met, but the maximum 8–hour average exceeds 160 μg m^{-3}, the MDA8 O_3 is still valid. We define the days with observed MDA8 O_3 concentrations higher than 160 μg m^{-3} as the heavy ozone pollution days, according to the Grade II standard of ambient air quality in China (MEE, 2012).

2.3. Classification of circulations

Identifying the typical circulation characteristics during pollution episodes could assist in the forecast of ozone pollution (Dong et al., 2020; Zhao et al., 2021). T–PCA approach is a widely used and objective classification method of circulations situation, which has high temporal and spatial stability and low dependence on preset parameters. The cost733 software is applied to realize T–PCA weather classification in the present study. Previous research has shown that ozone pollution in the YRD is mainly related to surface meteorological factors, 850 hPa wind (Dang et al., 2021), and frequently affected by the Western Pacific subtropical high (Shu et al., 2016; Gao et al., 2021). Following the previous studies (Li et al., 2019c; Gao et al., 2020; Mao et al., 2020; Miao et al., 2021; Ye et al., 2016), we thus use the geopotential heights on 850 hPa and 500 hPa levels, as well as sea level pressures for the circulation classification. The meteorological data is provided by the ERA5 reanalysis data of the European Centre for Medium–Range Weather Forecasts (ECMWF, https://cds.climate.copernicus.eu/cdsapp#!/dataset/reanalysis-era5-pressure-levels?tab=overview). The input data is in the East Asia region (20°–70°N, 70°–130°E) with a horizontal resolution of 0.25° × 0.25° and a temporal resolution of 6 h. The raw data of four times a day (0:00, 06:00, 12:00, 18:00 UTC) are averaged and standardized spatially before inputting into the cost733 software for classification, following the method by Li et al. (2019c) and Mao et al. (2020). In the present study, we would like to help predict typical ozone pollution events in different seasons and analyze the corresponding pollution characteristics, and thus haven't removed the seasonal pattern in the decomposition.

3. Results

3.1. Validation of simulated ozone

Fig. 1a shows the spatial distributions of observed and GEOS–Chem model simulated MDA8 O_3 concentrations averaged for May–July 2017. The observations are the average concentrations of monitoring stations in each city. The simulated and observed MDA8 O_3 concentrations are both 127 μg m^{-3} averaged in central and eastern China (18°–45°N, 97.5°–125°E) from May to July 2017 and the corresponding correlation coefficient (r) is 0.77 (95 % confidence level). The spatial distributions of simulated and observed ozone pollution are consistent and the ozone pollution level gradually decreases from the northeast to the southwest of China, which is consistent with results of previous studies (Lei et al.,

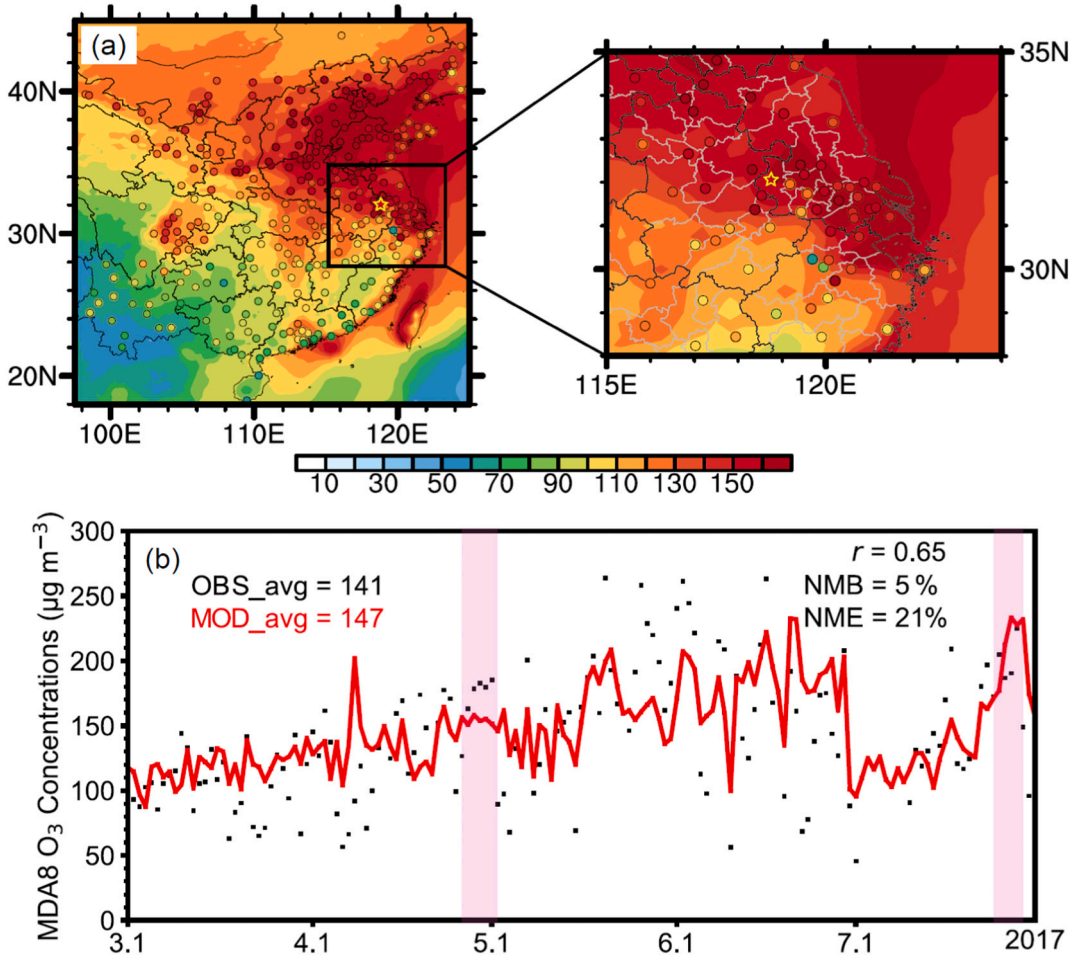

Fig. 1. (a) Observed and simulated average MDA8 O_3 concentrations in central and eastern China from May to July 2017. The yellow star indicates the location of Nanjing. (b) Time series of observed and simulated MDA8 O_3 in Nanjing from March to July 2017. The averages of observations and simulations in Nanjing from March to July, as well as their correlation coefficient (*r*), normalized mean bias (NMB), and normalized mean error (NME) are inserted. The pink shades represent the heavy ozone pollution events under the typical circulation patterns for adjoint simulations.

2022; Liu and Wang, 2020a; Wang et al., 2022a). The most serious ozone pollution region is the North China Plain with MDA8 O_3 concentrations exceeding 160 μg m^{-3} in most cities. In the YRD, the ozone pollution spatially shows a decrease trend from north to south. The MDA8 O_3 concentrations in several cities in the north of the YRD exceed 160 μg m^{-3} averaged from May to July 2017, and the pollutions in the south of the YRD are relatively light. Nanjing is located in the central area of the YRD and the MDA8 O_3 concentrations also reach 159 μg m^{-3}.

Fig. 1b shows the time series of the observed and GEOS–Chem simulated MDA8 O_3 concentrations in Nanjing from March to July 2017. The observations are the averages of ozone concentrations at 9 monitoring stations in Nanjing and the simulations are the average concentrations of the model grids corresponding to the monitoring stations. The observations show that the MDA8 O_3 gradually increase from March to June in Nanjing. Nevertheless, the plum rain season in early July may alleviate the ozone pollution in Nanjing, and the concentrations increase again after the plum rain (Xian et al., 2020). The trend of simulated MDA8 O_3 is consistent with the observations in Nanjing. In order to evaluate the performance of model simulations of MDA8 O_3, Emery et al. (2017) suggested that the model simulations are acceptable with the *r*, normalized mean bias (NMB) and normalized mean error (NME) between model simulations and observations of MDA8 O_3 >0.50, <15 % and 25 %, respectively. The simulated MDA8 O_3 are within the acceptable range, as the *r*, NMB, and NME of simulated and observed MDA8 O_3 in Nanjing from March to July 2017 are 0.65 (95 % confidence level), 5 %, and 21 %, respectively.

However, the GEOS-Chem adjoint model could not perfectly capture the observed high-level ozone concentrations and tends to overestimate the low-level ozone observations, which have also been reported by previous studies (e.g., Qu et al., 2020). For heavy ozone pollution days, there are 53 days with observed MDA8 O_3 >160 μg m^{-3} in Nanjing from March to July 2017, among which 19 days (16 days in spring) are not simulated to be in exceedance by the model. In these 19 days, the difference between the simulations and observations ranges from −32 % to −7 %. For 14 days (9 days in summer), the MDA8 O_3 concentrations are simulated exceeding 160 μg m^{-3} but not actually observed. For March–July 2017, there are 57 light pollution days (observed MDA8 O_3 between 100 and 160 μg m^{-3}) in Nanjing, among which 46 days are accurately simulated as light polluted. The deficiency of the model may be partially due to the uncertainties in emissions of ozone precursors and the chemical and physical process in the model simulations (Qu et al., 2020; Goldstein et al., 2004; Zhang et al., 2009).

3.2. *Dominant synoptic patterns of ozone pollution*

Weather circulations are classified on the 391 heavy ozone pollution days (observed MDA8 O_3 concentrations ≥160 μg m^{-3}) in Nanjing from April 2013 to December 2019. The cost733 software classifies the circulation patterns into 3 to 11 types (Fig. S2). Based on the studies of Huth et al. (2008) and Philipp et al. (2010), we select the circulation classification scheme of four types as the change in explained variation and pseudo-F value outputted in cost733 are relatively large. The

circulation patterns of heavy ozone pollution days are thus divided into four types by using the T–PCA method: LBH (Lake Balkhash High), ST_W (Siberian Trough in the west), SH (Siberian High) and NL (Northeast Low).

Fig. 2 shows the seasonal occurrence frequency of four types of synoptic patterns corresponding to the heavy ozone pollution days during April 2013 to December 2019. The results show that heavy ozone pollution in Nanjing mainly occurs in spring and summer, consistent with previous studies (Liu et al., 2020a; Mao et al., 2022a; Mao et al., 2022b; Yang et al., 2021), which is largely due to the increase in temperature, radiation and resulting photochemical reactions. According to the classification results, the different types of circulation patterns generally occur in different seasons, containing seasonal information of meteorological data, which would be conducive to the auxiliary prediction of ozone pollution in different seasons. The type LBH and type ST_W are the most important circulation patterns, accounting for 74 % of the heavy ozone pollution days in Nanjing. The type LBH (49 % frequency of occurrence) is the dominant synoptic pattern of the heavy ozone pollution days and mostly appears in March–April–May (MAM) and September–October–November (SON). The type LBH occurring in May, April and September accounts for 21 %, 11 % and 7 % of the total heavy pollution days, respectively. The type ST_W (25 % frequency of occurrence) only occurring in the warm season from May to August accounts for 1 %, 9 %, 9 % and 6 % of the total heavy pollution days, respectively. The type NL (16 % frequency of occurrence) and type SH mainly occur from May to September and the occurrence frequency of the type SH is the lowest (10 %).

Fig. S3 shows the typical circulation patterns of heavy ozone pollution days from April 2013 to December 2019, in which Fig. S3a shows the sea level pressure and 10 m wind field, Fig. S3b and S3c show the geopotential height and corresponding wind fields at 850 hPa and 500 hPa levels. The type LBH is the dominant circulation patterns in heavy ozone pollution days, characterized by the Balkhash high, the Northeast China low, and the Yellow Sea high. In the type ST_W, the trough is anomalously located over the West Siberian and the Yellow Sea is controlled by a weak high. For the type LBH and the type ST_W, the YRD is at the bottom of Yellow Sea high and controlled by the high–pressure system which is conducive to the development of fine weather with high temperature and low humidity and thus is favorable for the formation of ozone. In two main types, the type LBH and the type ST_W, the YRD is affected by the southeast wind at the surface and 850 hPa level, which probably cause the transport of ozone and its precursors emitted from the southeastern YRD region. The type SH and the type NL have the similar characteristics of circulation patterns with the Siberian High and the Northeast China Low. The Siberian high in the type SH moves eastward and is stronger than that in the type NL, and the Northeast China low is weaker in the type SH than in the type NL. A weak high appears in the Yellow Sea, which is favorable to the formation of sunny weather in the YRD.

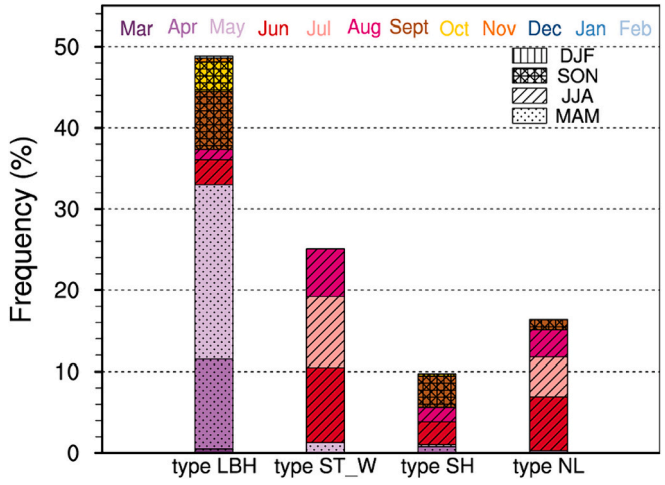

Fig. 2. Frequency of circulation types of heavy ozone pollution days in Nanjing in each month and season from April 2013 to December 2019. Different colors represent different months, and shades of different shapes represent different seasons.

3.3. Typical heavy ozone pollution events

Following previous studies (Chang et al., 2021; Mao et al., 2020; Xiao et al., 2020; Zong et al., 2023), we analyze the heavy ozone pollution events corresponding to the typical circulation patterns. To ensure the results more representative, we select the pollution events for the adjoint simulations based on the following criteria: heavy ozone pollution occurred for 4 consecutive days or more under the same circulation pattern; the differences between the simulated and the observed surface ozone concentrations in the selected events are within 25 %. Two typical heavy ozone pollution events in Nanjing are thus selected from April 27 to May 1, 2017 under the type LBH in spring, and from July 25 to July 28, 2017 under the type ST_W in summer, The daily circulation patterns (Figs. S4 and S5) of the two events are basically consistent with the average circulation patterns (Fig. S3) obtained by classification. The heavy ozone pollution events in the type SH and the type NL are not included in the present study, as the frequencies of the two types are low and the continuous heavy ozone pollution days in the same type are basically few.

Fig. 3 shows the sensitivities of surface ozone in Nanjing to NO_x, CO and NMVOCs emissions emitted from anthropogenic and biomass burning sources during the heavy ozone pollution event of circulation type LBH from April 27 to May 1, 2017. The GEOS–Chem adjoint model is integrated backward for >40 days. As previous studies have shown that the emissions from biomass burning sources could increase ozone concentrations in the YRD (Liu et al., 2022b; Xu et al., 2018), the ozone sensitivities in Nanjing to precursors emitted from biomass burning sources are also calculated in this study. The sensitivities represent the changes of ozone concentrations in Nanjing for a 10 % increase in emissions at model grids under the condition of constant chemical environment, following the study by Wang et al. (2021b). Fig. 4 indicates the changes of ozone concentrations in Nanjing caused by the 10 % increase in the emissions of ozone precursors emitted from different regions, and Fig. S6 shows the region division.

According to Fig. 3, the sensitivities of ozone in Nanjing to anthropogenic and biomass burning emissions in the YRD show a similar spatial distribution. The sensitivities of ozone in Nanjing to local NO_x emissions are negative, indicating that the increase in NO_x emissions in Nanjing could reduce local ozone pollution; in other words, the reduction of NO_x emissions in Nanjing would thus aggravate local pollution. The ozone sensitivities in Nanjing to NO_x emissions are generally positive in eastern China, but negative in the highly polluted regions in the YRD, e.g., southern Jiangsu, Shanghai and Hangzhou, where are mainly under a NMVOCs–limited regime in the spring of 2017 (Ding et al., 2019; Mao et al., 2022b; Wang et al., 2019b). The sensitivities of ozone in Nanjing to CO and NMVOCs emissions in eastern China are positive, and thus the reduction of the NMVOCs and CO emissions could effectively alleviate ozone pollution in Nanjing. In addition, the sensitivities of ozone in Nanjing to its precursor emissions are high in Zhejiang and southern Jiangsu, which shows that emissions from the south and southeast of Nanjing contribute significantly to the ozone pollution in Nanjing. The result is consistent with the dominant wind of Nanjing (Fig. S3), which is southeasterly at the surface and southerly at 850 hPa for circulation type LBH.

For anthropogenic emissions, the sensitivities of ozone in Nanjing to a 10 % increase in anthropogenic NO_x emissions would be 0.83 μg m^{-3} for the whole of China (Table S1), −0.18 μg m^{-3} in Nanjing, −0.69 μg m^{-3} in Jiangsu (except Nanjing), and 0.98 μg m^{-3} in Zhejiang (including Shanghai). For different sectors of anthropogenic emissions, NO_x

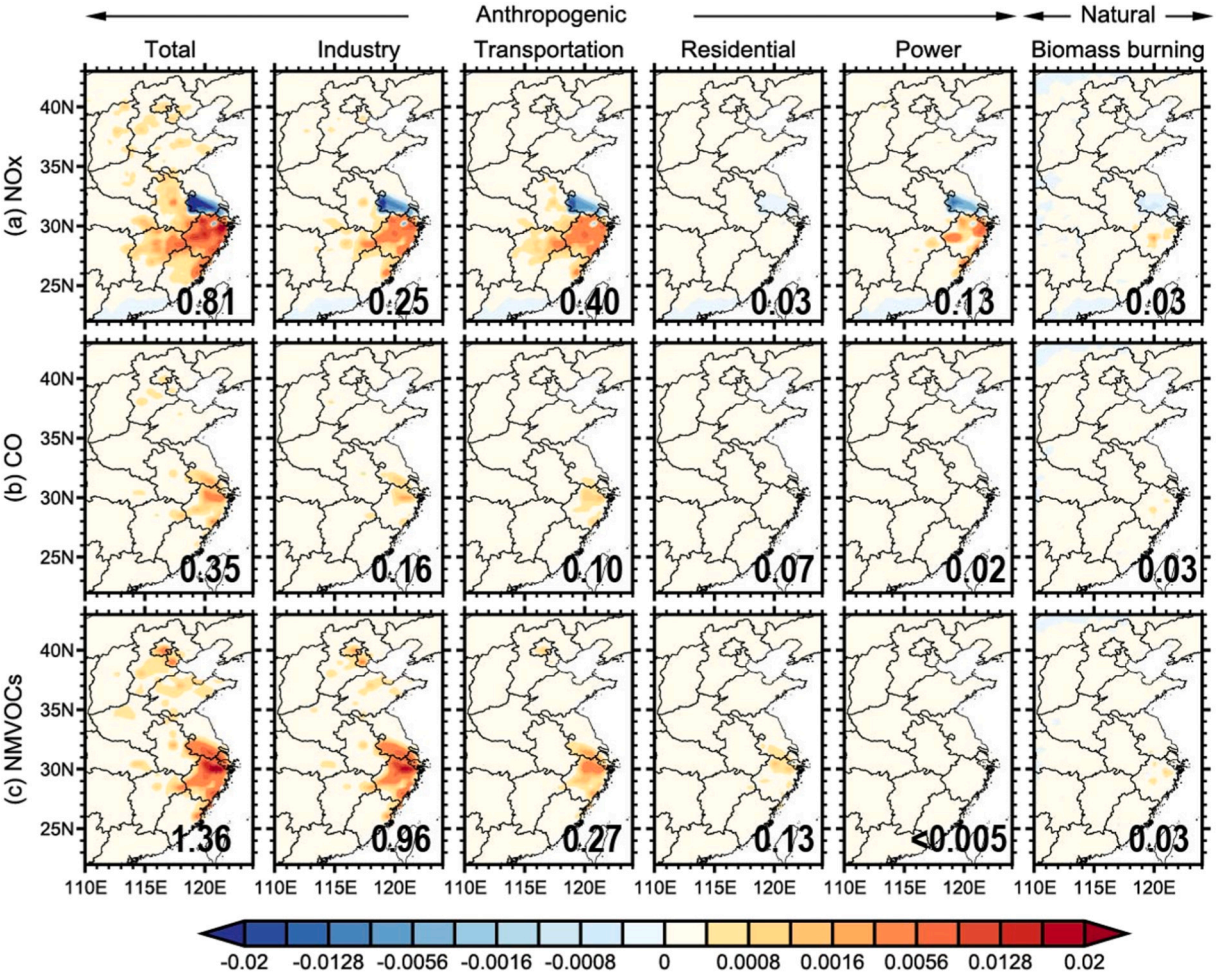

Fig. 3. Sensitivities of ozone (μg m^{-3}) to a 10 % increase in NO_x, CO and NMVOCs emissions in the heavy ozone pollution event of type LBH from April 27 to May 1, 2017. Sensitivities of ozone to anthropogenic emissions are separated by sectors. The positive sensitivity areas indicate that the precursor emission reduction in those areas could effectively alleviate the ozone pollution in Nanjing. The values represent the total sensitivities of ozone to its precursor emissions in the region.

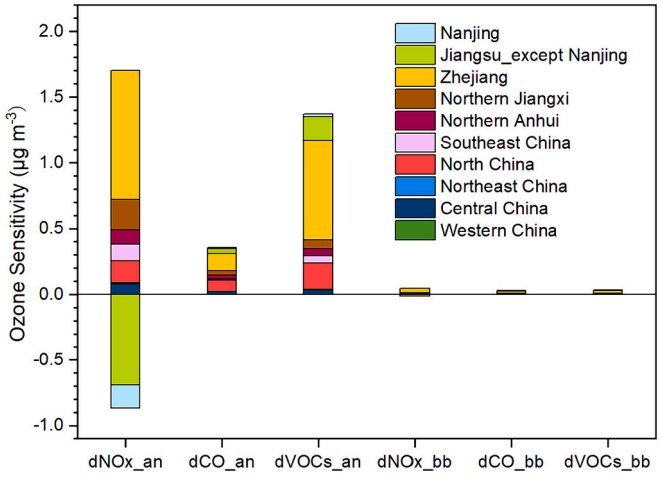

Fig. 4. Sensitivities of ozone (μg m^{-3}) in Nanjing to a 10 % increase in NO_x, CO and NMVOCs emissions in different regions of China in heavy ozone pollution event of type LBH from April 27 to May 1, 2017 (the suffix "an" in the figure represents the anthropogenic emission, and "bb" represents the biomass burning emission).

emissions from industry and transportation sectors in Eastern China substantially affect ozone concentrations in Nanjing. By summed the ozone sensitivities to emissions from different emission sectors shown in Fig. 3, the ozone sensitivities to a 10 % increase in anthropogenic NO_x emissions from industry sector are −0.08 μg m^{-3} in Nanjing, −0.31 μg m^{-3} in Jiangsu (except Nanjing), and 0.37 μg m^{-3} in Zhejiang; for transportation sector, the corresponding sensitivities are −0.07 μg m^{-3}, −0.23 μg m^{-3}, and 0.40 μg m^{-3}, respectively. For power sector, the sensitivities of ozone in Nanjing caused by the 10 % increase in NO_x power emissions in China are only 0.14 μg m^{-3}; the NO_x emissions from power sector in Jiangsu and Zhejiang have a relatively high impact on the ozone pollution in Nanjing, and the ozone sensitivities are −0.18 μg m^{-3} and 0.20 μg m^{-3}, respectively.

Different from the influence of NO_x emissions on ozone, the reduction of anthropogenic NMVOCs emissions in various regions would abate the ozone pollution in Nanjing. The sensitivities of ozone concentrations in Nanjing caused by the 10 % increase of anthropogenic NMVOCs emissions in the locality, Jiangsu (except Nanjing), Zhejiang and North China are 0.02 μg m^{-3}, 0.18 μg m^{-3}, 0.75 μg m^{-3} and 0.20 μg m^{-3}, respectively. For different sectors of anthropogenic emissions, the NMVOCs emissions from industry sector account for about 70 % of the impact of anthropogenic NMVOCs on ozone pollution. The ozone sensitivities to NMVOCs emissions from industry sector are 0.55 μg m^{-3} in Zhejiang and 0.14 μg m^{-3} in Jiangsu. In addition, the ozone sensitivities in Nanjing to a 10 % increase in NMVOCs emissions from transportation sector are 0.15 μg m^{-3} in Zhejiang and only 0.04 μg m^{-3} in Jiangsu. The

ozone sensitivities in Nanjing to anthropogenic CO emissions are lower compared with those to NO_x and NMVOCs emissions. The sensitivities of ozone concentrations in Nanjing to a 10 % increase in anthropogenic CO emissions are 0.35 μg m^{-3} in China, 0.13 μg m^{-3} in Zhejiang, 0.08 μg m^{-3} in North China and 0.05 μg m^{-3} in Jiangsu. For different emission sectors, industry and transportation sectors in China have a high impact on ozone in Nanjing, contributing 45 % and 29 % of the ozone sensitivities to anthropogenic CO emissions, respectively.

For the natural source, the impact of biomass burning emissions on ozone in Nanjing is far less than that of anthropogenic emissions. The ozone sensitivities in Nanjing caused by a 10 % increase in NO_x, CO and NMVOCs biomass burning emissions in China are only 0.04 μg m^{-3}, 0.03 μg m^{-3} and 0.04 μg m^{-3}, respectively. The ozone sensitivities in Nanjing to the biogenic emission of isoprene (Fig. S7) and soil NO_x emission (Fig. S8) are also low and the relatively high sensitivities are only about 0.05 μg m^{-3} in Zhejiang (Fig. S7), which implies that the contributions of anthropogenic precursors to ozone in the YRD are much larger than those of natural precursors during the heavy ozone pollution days (Fan et al., 2021).

Figs. 5 and 6 show the ozone sensitivities in Nanjing to a 10 % increase of ozone precursors emissions during the heavy ozone pollution event from July 25 to July 28, 2017 for circulation type ST_W. The ozone sensitivities to local precursor emissions in Nanjing are similar to that of heavy pollution event for circulation type LBH. The ozone sensitivities to NO_x emissions in Nanjing are negative, and the sensitivities to local CO and NMVOCs emissions are positive, which indicates that the reduction of CO and NMVOCs emissions would mitigate ozone concentrations in Nanjing, and the reduction of NO_x emissions would have the opposite effect. However, unlike the heavy pollution for the type LBH, the reduction of ozone precursors emissions in Jiangsu (except Nanjing) and Zhejiang could both significantly reduce the ozone pollution in Nanjing for the type ST_W. In addition, NO_x emission reductions in northern Anhui and northern Henan could also lightly reduce ozone pollution in

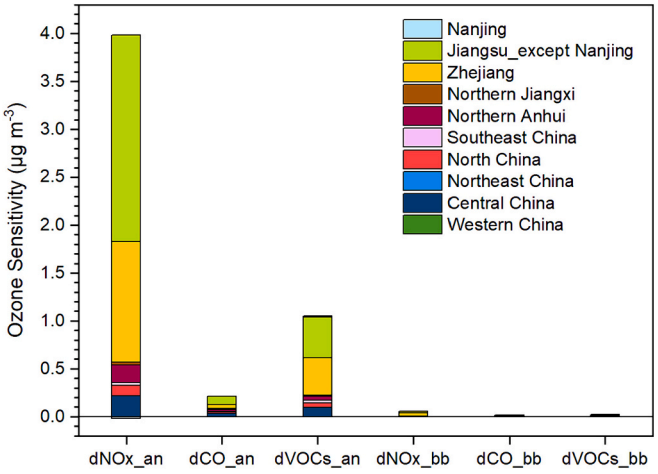

Fig. 6. Same as Fig. 4, but in heavy ozone pollution event in Nanjing of type ST_W from July 25 to July 28, 2017.

Nanjing. The ozone concentrations in Nanjing are mainly affected by the emissions from the southeast of Nanjing (southern Jiangsu and northern Zhejiang), mainly due to the southeast wind at ground level in Nanjing and at 850 hPa for circulation type ST_W. The differences in the sensitivities results from the two heavy ozone pollution events are possibly related to the circulation classification that the types LBH mainly appears in spring and the type ST_W is in summer. From the spring to the summer 2017, the highly polluted regions in the YRD gradually transition from the NMVOCs–limited area to NMVOCs–NO_x–limited area (Ding et al., 2019; Mao et al., 2022b; Wang et al., 2019b; Wang et al., 2022a). The sensitivities in the YRD are generally larger in the type ST_W than in the type LBH, likely due to the increased temperature and

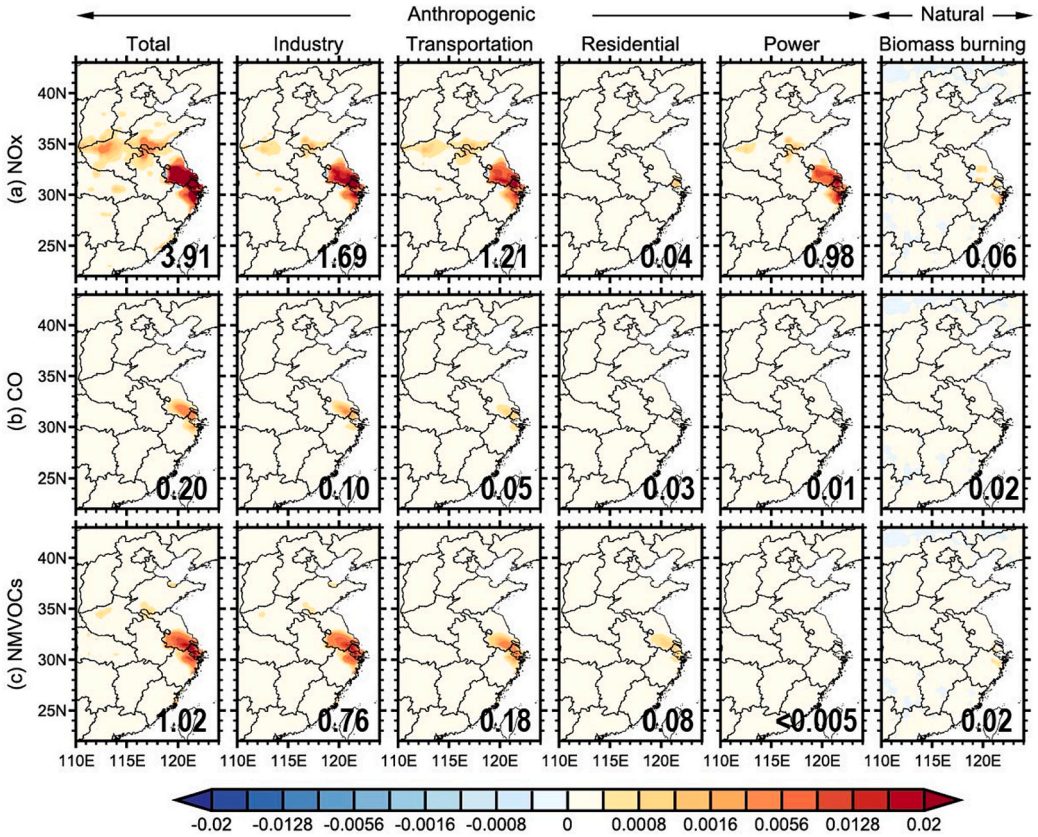

Fig. 5. Same as Fig. 3, but in heavy ozone pollution event in Nanjing of type ST_W from July 25 to July 28, 2017.

enhanced radiation in summer, and resulting enhanced photochemical reactions.

The sensitivities of ozone concentrations in Nanjing caused by a 10 % increase in anthropogenic NO_x emissions are −0.02 μg m^{-3} in the locality, 2.16 μg m^{-3} in Jiangsu (except Nanjing), 1.26 μg m^{-3} in Zhejiang (including Shanghai), 0.18 μg m^{-3} in northern Anhui and 0.22 μg m^{-3} in central China (Table S2). As for different emission sectors, industry sector in China accounts for 43 % of the ozone sensitivities in Nanjing to the total anthropogenic NO_x emissions, followed by transportation sector (31 %) and power sector (25 %). The ozone sensitivities to the NO_x emissions from industry sector are 0.96 μg m^{-3} in Jiangsu and 0.53 μg m^{-3} in Zhejiang; those from transportation sector and power sector are 0.65 μg m^{-3} and 0.51 μg m^{-3} in Jiangsu, and 0.34 μg m^{-3} and 0.37 μg m^{-3} in Zhejiang. The ozone sensitivities in Nanjing to a 10 % increase in NO_x emission from residential sector in China are only 0.04 μg m^{-3}.

Similar to anthropogenic NO_x emissions, anthropogenic NMVOCs emissions from Jiangsu (except Nanjing) and Zhejiang have the significantly impact on ozone pollution in Nanjing, with sensitivities of 0.43 μg m^{-3} and 0.39 μg m^{-3}, respectively. The ozone sensitivities to a 10 % increase in local anthropogenic NMVOCs emissions in Nanjing are only 0.01 μg m^{-3}. For different sectors of anthropogenic emissions, the contributions of NMVOCs emissions from industry sector to ozone pollution in Nanjing account for above 70 %. The ozone sensitivities in Nanjing caused by a 10 % increase in NMVOCs emissions emitted from industry sector are 0.33 μg m^{-3} in Jiangsu and 0.30 μg m^{-3} in Zhejiang, and those from transportation sector are both 0.07 μg m^{-3}. The ozone sensitivities in Nanjing to a 10 % increase in anthropogenic CO emissions in China are only 0.21 μg m^{-3}. For different emission sectors, the sensitivities to CO emissions from industry sector are relatively large, about 0.10 μg m^{-3} in China, 0.05 μg m^{-3} in Jiangsu, and 0.02 μg m^{-3} in Zhejiang. For natural emissions, the ozone sensitivities to precursors emissions emitted from biomass burning sources and biogenic sources (Fig. S7) and soil sources (Fig. S8) are substantially less than those from anthropogenic sources for the type ST_W, which is similar to the result for the type LBH.

4. Conclusions

In the present study, GEOS–Chem and its adjoint model were used to quantify the sensitivities of ozone to its precursor emissions from different source regions and emission sectors during the heavy ozone pollution events in the YRD. We used GEOS–FP assimilated data with a horizontal resolution of 0.25° × 0.3125° to drive model simulation, and the MEIC anthropogenic emission inventory in China. The simulated MDA8 O_3 in GEOS–Chem adjoint model were acceptable, as the *r*, NMB and NME of simulated and observed MDA8 O_3 at 2 m height above the surface were 0.65 (95 % confidence level), 5 % and 21 %, respectively, in Nanjing from March to July 2017.

The circulation patterns of heavy ozone pollution days in Nanjing were also classified by using the T–PCA classification method from April 2013 to December 2019. During heavy ozone pollution days, Nanjing was mostly controlled by high pressure and southeast wind at the surface and 850 hPa level. The type LBH and type ST_W were the main circulation types, mainly appeared in spring and summer. The type LBH occurred in May and type ST_W in summer accounted for 21 % and 24 % of the total heavy pollution days, respectively.

During the heavy ozone pollution event of type LBH in spring, the reduction of anthropogenic NMVOCs and NO_x emissions in Zhejiang and the reduction of anthropogenic NMVOCs emissions in the YRD would effectively reduce ozone pollution in Nanjing. Especially in Zhejiang, the 10 % reduction of anthropogenic NO_x and NMVOCs emissions could reduce the ozone concentrations in Nanjing by 0.98 μg m^{-3} and 0.75 μg m^{-3}, respectively. For type ST_W that occurs mainly in summer, when the anthropogenic NO_x emissions in Jiangsu, Zhejiang and Shanghai decreased by 10 %, the ozone concentrations in Nanjing would considerably decrease by 3.40 μg m^{-3}. For different emission sectors, industry sector accounted for 31 %–74 % of the ozone sensitivities in Nanjing to total anthropogenic emissions in China, followed by transportation sector (18 %–49 %).

Identifying the characteristics of the large-scale circulation during the heavy ozone pollution events could provide a basis for the prediction of ozone pollution. When the typical synoptic patterns occur, the adjoint analysis of ozone precursor sources would help further formulate accurate emission reduction measures, which could be implemented in advance to prevent the occurrence of heavy ozone pollution. Currently, only two ozone pollution events have been selected for study, and more ozone pollution events in different circulation types would further analyze in future research to obtain more general conclusions about the ozone sensitivities to its precursor emissions. And we would like to extend the research area to the eastern China and include temporal variations of impact of regional transport on ozone pollution (Mao et al., 2020; Zhang et al., 2009) in the following work. Notably, the results of the adjoint method are highly dependent on the accuracy of model simulation (Jiang et al., 2015; Wang et al., 2019c) and the emission inventories (Wang et al., 2021b).

CRediT authorship contribution statement

Yu-Hao Mao: Writing – review & editing, Supervision, Methodology, Conceptualization. **Yongjie Shang:** Writing – original draft, Visualization, Formal analysis. **Hong Liao:** Conceptualization. **Hansen Cao:** Methodology. **Zhen Qu:** Methodology. **Daven K. Henze:** Methodology.

Declaration of competing interest

The authors declare that they have no competing financial interests or personal relationships that could have appeared to influence the work reported in this paper.

Data availability

Data will be made available on request.

Acknowledgments

This work was supported by Major Program of National Natural Science Foundation of China (grant no. 42293320), Natural Science Foundation of Jiangsu Province (grant no. BK20220031) and the China Postdoctoral Science Foundation (2017M620218, 2018T110526). We acknowledge the High-Performance Computing Centre of Nanjing University of Information Science and Technology for their support of this work.

Appendix A. Supplementary data

Supplementary data to this article can be found online at https://doi.org/10.1016/j.scitotenv.2024.171585.

References

Bey, I., Jacob, D., Yantosca, R., Logan, J., Field, B., Fiore, A., Li, Q.-B., Liu, H., Mickley, L., Schultz, M., 2001. Global modeling of tropospheric chemistry with assimilated meteorology: model description and evaluation. J. Geophys. Res. Atmos. 106 https://doi.org/10.1029/2001JD000807.

Chang, L., He, F., Tie, X., Xu, J., Gao, W., 2021. Meteorology driving the highest ozone level occurred during mid-spring to early summer in Shanghai, China. Sci. Total Environ. 785 https://doi.org/10.1016/j.scitotenv.2021.147253.

Chen, X., Jiang, Z., Shen, Y., Li, R., Fu, Y., 2021. Chinese regulations are working—why is surface ozone over industrialized areas still high? Applying lessons from northeast US air quality evolution. Geophys. Res. Lett. 48 https://doi.org/10.1029/2021GL092816.

Dang, R., Liao, H., Fu, Y., 2021. Quantifying the anthropogenic and meteorological influences on summertime surface ozone in China over 2012–2017. Sci. Total Environ. 754, 142394 https://doi.org/10.1016/j.scitotenv.2020.142394.

Ding, D., Xing, J., Wang, S., Chang, X., Hao, J., 2019. Impacts of emissions and meteorological changes on China's ozone pollution in the warm seasons of 2013 and 2017. Front. Environ. Sci. Eng. 13, 1–9. https://doi.org/10.1007/s11783-019-1160-1.

Dong, Y., Li, J., Guo, J., Jiang, Z., Chu, Y., Chang, L., Yang, Y., Liao, H., 2020. The impact of synoptic patterns on summertime ozone pollution in the North China Plain. Sci. Total Environ. 735, 139559 https://doi.org/10.1016/j.scitotenv.2020.139559.

Emery, C., Liu, Z., Russell, A.G., Odman, M.T., Yarwood, G., Kumar, N., 2017. Recommendations on statistics and benchmarks to assess photochemical model performance. J. Air Waste Manage. Assoc. 67 (5), 582–598. https://doi.org/10.1080/10962247.2016.1265027.

Fan, M., Zhang, Y., Lin, Y., Li, L., Xie, F., Hu, J., Mozaffar, A., Cao, F., 2021. Source apportionments of atmospheric volatile organic compounds in Nanjing, China during high ozone pollution season. Chemosphere 263, 128025. https://doi.org/10.1016/j.chemosphere.2020.128025.

Fang, T., Zhu, Y., Wang, S., Xing, J., Zhao, B., Fan, S., Li, M., Yang, W., Chen, Y., Huang, R., 2021. Source impact and contribution analysis of ambient ozone using multi-modeling approaches over the Pearl River Delta region, China. Environ. Pollut. 289, 117860 https://doi.org/10.1016/j.envpol.2021.117860.

Feng, Z., Xu, Y., Kobayashi, K., Dai, L., Zhang, T., Agathokleous, E., Calatayud, V., Paoletti, E., Mukherjee, A., Agrawal, M., Park, R., Oak, Y., Yue, X., 2022. Ozone pollution threatens the production of major staple crops in East Asia. Nat. Food 3, 47–56. https://doi.org/10.1038/s43016-021-00422-6.

Fu, Y., Liao, H., Yang, Y., 2019. Interannual and decadal changes in tropospheric ozone in China and the associated chemistry-climate interactions: a review. Adv. Atmos. Sci. 36 (9), 975–993. https://doi.org/10.1007/s00376-019-8216-9.

Gao, W., Tie, X., Xu, J., Huang, R., Mao, X., Zhou, G., Chang, L., 2017. Long-term trend of O_3 in a mega City (Shanghai), China: characteristics, causes, and interactions with precursors. Sci. Total Environ. 603–604, 425–433. https://doi.org/10.1016/j.scitotenv.2017.06.099.

Gao, D., Xie, M., Chen, X., Wang, T., Liu, J., Xu, Q., Mu, X., Chen, F., Li, S., Zhuang, B., Li, M., Zhao, M., Ren, J., 2020. Systematic classification of circulation patterns and integrated analysis of their effects on different ozone pollution levels in the Yangtze River Delta Region, China. Atmos. Environ. 242 https://doi.org/10.1016/j.atmosenv.2020.117760.

Gao, D., Xie, M., Liu, J., Wang, T., Ma, C., Bai, H., Chen, X., Li, M., Zhuang, B., Li, S., 2021. Ozone variability induced by synoptic weather patterns in warm seasons of 2014–2018 over the Yangtze River Delta region, China. Atmos. Chem. Phys. 21 (8), 5847–5864. https://doi.org/10.5194/acp-21-5847-2021.

Ge, S., Wang, S., Xu, Q., Ho, T., 2021. Source apportionment simulations of ground-level ozone in Southeast Texas employing OSAT/APCA in CAMx. Atmos. Environ. 253 https://doi.org/10.1016/j.atmosenv.2021.118370.

Goldstein, A.H., Millet, D.B., McKay, M., Jaegle', L., Horowitz, L., Cooper, O., Hudman, R., Jacob, D.J., Oltmans, S., Clarke, A., 2004. Impact of Asian emissions on observations at Trinidad Head, California, during ITCT 2K2. J. Geophys. Res. 109, D23S17 https://doi.org/10.1029/2003JD004406.

Gong, X., Hong, S., Jaffe, D.A., 2018. Ozone in China: spatial distribution and leading meteorological factors controlling O_3 in 16 Chinese cities. Aerosol Air Qual. Res. 18 (9), 2287–2300. https://doi.org/10.4209/aaqr.2017.10.0368.

Guenther, A., Jiang, M., Heald, C., Sakulyanontvittaya, Duhl, T., Emmons, L., Wang, J., 2012. The model of emissions of gases and aerosols from nature version 2.1 (MEGAN2.1): an extended and updated framework for modeling biogenic emissions. Geosci. Model Dev. Discuss. 5, 1–58. https://doi.org/10.5194/gmdd-5-1-2012.

Henze, D.K., Hakami, A., Seinfeld, J.H., 2007. Development of the adjoint of GEOS-Chem. Atmos. Chem. Phys. 7, 2413–2433.

Henze, D.K., Seinfeld, J.H., Shindell, D.T., 2009. Inverse modeling and mapping US air quality influences of inorganic $PM_{2.5}$ precursor emissions using the adjoint of GEOS-Chem. Atmos. Chem. Phys. 9, 5877–5903.

Huang, J.-P., Fung, J.C.H., Lau, A.K.H., 2006. Integrated processes analysis and systematic meteorological classification of ozone episodes in Hong Kong. J. Geophys. Res. 111 (D20) https://doi.org/10.1029/2005jd007012.

Hudman, R., Russell, A., Valin, L., Cohen, R., 2010. Interannual variability in soil nitric oxide emissions over the United States as viewed from space. Atmos. Chem. Phys. Discuss. 10 https://doi.org/10.5194/acpd-10-13029-2010.

Hudman, R., Moore, N., Mebust, A., Martin, R., Russell, A., Valin, L., Cohen, R., 2012. Steps towards a mechanistic model of global soil nitric oxide emissions: implementation and space based-constraints. Atmos. Chem. Phys. 12, 7779–7795. https://doi.org/10.5194/acp-12-7779-2012.

Hung, C.-H., Lo, K.-C., 2015. Relationships between ambient ozone concentration changes in southwestern Taiwan and invasion tracks of tropical typhoons. Adv. Meteorol. 2015, 1–17. https://doi.org/10.1155/2015/402976.

Huth, R., Beck, C., Philipp, A., Demuzere, M., Ustrnul, Z., Cahynova, M., Kyselý, J., Tveito, O.E., 2008. Classifications of atmospheric circulation patterns: recent advances and applications. Ann. N. Y. Acad. Sci. 1146, 105–152. https://doi.org/10.1196/annals.1446.019.

Jiang, Z., Worden, J.R., Jones, D.B.A., Lin, J.T., Verstraeten, W.W., Henze, D.K., 2015. Constraints on Asian ozone using Aura TES, OMI and Terra MOPITT. Atmos. Chem. Phys. 15 (1), 99–112. https://doi.org/10.5194/acp-15-99-2015.

Lapina, K., Henze, D., Milford, J., Travis, K., 2015. Impacts of foreign, domestic and state-level emissions on ozone-induced vegetation loss in the U.S. Environ. Sci. Technol. 50 https://doi.org/10.1021/acs.est.5b04887.

Lei, Y., Yue, X., Wang, Z., Liao, H., Zhang, L., 2022. Mitigating ozone damage to ecosystem productivity through sectoral and regional emission controls: a case study in the Yangtze River Delta, China. Environ. Res. Lett. 17 https://doi.org/10.1088/1748-9326/ac6ff7.

Li, L., An, J., Huang, L., Yan, R., Huang, C., Yarwood, G., 2019a. Ozone source apportionment over the Yangtze River Delta region, China: investigation of regional transport, sectoral contributions and seasonal differences. Atmos. Environ. 202, 269–280. https://doi.org/10.1016/j.atmosenv.2019.01.028.

Li, B., Ho, S.S.H., Gong, S., Ni, J., Li, H., Han, L., Yang, Y., Qi, Y., Zhao, D., 2019b. Characterization of VOCs and their related atmospheric processes in a central Chinese city during severe ozone pollution periods. Atmos. Chem. Phys. 19 (1), 617–638. https://doi.org/10.5194/acp-19-617-2019.

Li, J., Liao, H., Hu, J., Li, N., 2019c. Severe particulate pollution days in China during 2013e2018 and the associated typical weather patterns in Beijing-Tianjin-Hebei and the Yangtze River Delta regions. Environ. Pollut. 248, 74–81. https://doi.org/10.1016/j.envpol.2019.01.124.

Liu, Y., Wang, T., 2020a. Worsening urban ozone pollution in China from 2013 to 2017 – part 1: the complex and varying roles of meteorology. Atmos. Chem. Phys. 20 (11), 6305–6321. https://doi.org/10.5194/acp-20-6305-2020.

Liu, Y., Wang, T., 2020b. Worsening urban ozone pollution in China from 2013 to 2017 – part 2: the effects of emission changes and implications for multi-pollutant control. Atmos. Chem. Phys. 20 (11), 6323–6337. https://doi.org/10.5194/acp-20-6323-2020.

Liu, L., Guo, J., Miao, Y., Liu, L., Li, J., Chen, D., He, J., Cui, C., 2018. Elucidating the relationship between aerosol concentration and summertime boundary layer structure in central China. Environ. Pollut. 241, 646–653. https://doi.org/10.1016/j.envpol.2018.06.008.

Liu, J., Wang, L., Li, M., Liao, Z., Sun, Y., Song, T., Gao, W., Wang, Y., Li, Y., Ji, D., Hu, B., Kerminen, V.-M., Wang, Y., Kulmala, M., 2019a. Quantifying the impact of synoptic circulation patterns on ozone variability in northern China from April to October 2013–2017. Atmos. Chem. Phys. 19 (23), 14477–14492. https://doi.org/10.5194/acp-19-14477-2019.

Liu, H., Zhang, M., Han, X., Li, J., Chen, L., 2019b. Episode analysis of regional contributions to tropospheric ozone in Beijing using a regional air quality model. Atmos. Environ. 199, 299–312. https://doi.org/10.1016/j.atmosenv.2018.11.044.

Liu, T., Wang, C., Wang, Y., Huang, L., Li, J., Xie, F., Zhang, J., Hu, J., 2020a. Impacts of model resolution on predictions of air quality and associated health exposure in Nanjing, China. Chemosphere 249, 126515. https://doi.org/10.1016/j.chemosphere.2020.126515.

Liu, H., Zhang, M., Han, X., 2020b. A review of surface ozone source apportionment in China. Atmos. Ocean. Sci. Lett. 13 (5), 470–484. https://doi.org/10.1080/16742834.2020.1768025.

Liu, X., Guo, H., Zeng, L., Lyu, X., Wang, Y., Zeren, Y., Yang, J., Zhang, L., Zhao, S., Li, J., Zhang, G., 2021. Photochemical ozone pollution in five Chinese megacities in summer 2018. Sci. Total Environ. 801, 149603 https://doi.org/10.1016/j.scitotenv.2021.149603.

Liu, Z., Lei, Y., Xue, W., Liu, X., Jiang, Y., Shi, X., Zheng, Y., Zhang, Q., Wang, J., 2022a. Mitigating China's ozone pollution with more balanced health benefits. Environ. Sci. Technol. 56 (12), 7647–7656. https://doi.org/10.1021/acs.est.2c00114.

Liu, Y., Zhao, H., Zhao, G., Xuelei, Z., Xiu, A., 2022b. Carbonaceous gas and aerosol emissions from biomass burning in China from 2012 to 2021. J. Clean. Prod. 362, 132199 https://doi.org/10.1016/j.jclepro.2022.132199.

Mao, J., Paulot, F., Jacob, D.J., Cohen, R.C., Crounse, J.D., Wennberg, P.O., Keller, C.A., Hudman, R.C., Barkley, M.P., Horowitz, L.W., 2013. Ozone and organic nitrates over the eastern United States: sensitivity to isoprene chemistry. J. Geophys. Res. Atmos. 118 (19), 11,256–11,268. https://doi.org/10.1002/jgrd.50817.

Mao, Y., Zhao, X., Liao, H., Zhao, D., Tian, P., Henze, D.K., Cao, H., Zhang, L., Li, J., Li, J., Ran, L., Zhang, Q., 2020. Sources of black carbon during severe haze events in the Beijing–Tianjin–Hebei region using the adjoint method. Sci. Total Environ. 740 https://doi.org/10.1016/j.scitotenv.2020.140149.

Mao, J., Li, L., Li, J., Sulaymon, I.D., Xiong, K., Wang, K., Zhu, J., Chen, G., Ye, F., Zhang, N., Qin, Y., Qin, M., Hu, J., 2022a. Evaluation of long-term modeling fine particulate matter and ozone in China during 2013–2019. Front. Environ. Sci. 10 https://doi.org/10.3389/fenvs.2022.872249.

Mao, Y., Yu, S., Shang, Y., Liao, H., Li, N., 2022b. Response of summer ozone to precursor emission controls in the Yangtze River Delta region. Front. Environ. Sci. 10 https://doi.org/10.3389/fenvs.2022.864897.

MEE (Ministry of Ecology and Environment of the People's Republic of China), 2012. Ambient air quality standards. Available at: https://www.mee.gov.cn/ywgz/fgbz/bz/bzwb/dqhjbh/dqhjzlbz/201203/W020120410330232398521.pdf.

MEE (Ministry of Ecology and Environment of the People's Republic of China), 2013. China environmental status bulletin. Available at: https://www.mee.gov.cn/hjzl/sthjzk/.

MEE (Ministry of Ecology and Environment of the People's Republic of China), 2019. China environmental status bulletin. Available at: https://www.mee.gov.cn/hjzl/sthjzk/.

Miao, Y., Liu, S., Huang, S., 2019. Synoptic pattern and planetary boundary layer structure associated with aerosol pollution during winter in Beijing, China. Sci. Total Environ. 682, 464–474. https://doi.org/10.1016/j.scitotenv.2019.05.199.

Miao, Y., Che, H., Zhang, X., Liu, S., 2021. Relationship between summertime concurring $PM_{2.5}$ and O_3 pollution and boundary layer height differs between Beijing and Shanghai, China. Environ. Pollut. 268 (Pt A), 115775 https://doi.org/10.1016/j.envpol.2020.115775.

Murray, L., Jacob, D., Logan, J., Hudman, R., Koshak, W., 2012. Optimized regional and interannual variability of lightning in a global chemical transport model constrained by LIS/OTD satellite data. J. Geophys. Res. Atmos. 117, 20307 https://doi.org/10.1029/2012JD017934.

NMEEB (Nanjing Municipal Ecology and Environment Bureau), 2016. Nanjing environmental status bulletin. Available at: http://sthjj.nanjing.gov.cn/njshjbhj/?id=xxgk_388.

NMEEB (Nanjing Municipal Ecology and Environment Bureau), 2019. Nanjing environmental status bulletin. Available at: http://sthjj.nanjing.gov.cn/njshjbhj/?id=xxgk_388.

Ott, L., Pickering, K., Stenchikov, G., Allen, D., DeCaria, A., Ridley, B., Lin, R.-F., Lang, S., Tao, W.-K., 2010. Production of lightning NOx and its vertical distribution calcuated from three-dimensional cloud-scale chemical transport model simulations. J. Geophys. Res. Atmos. 115 https://doi.org/10.1029/2009JD011880.

Park, R., Jacob, D., Field, B., Yantosca, R., 2004. Natural and transboundary pollution influences on sulfate-nitrate-ammonium aerosols in the United States: implications for policy. J. Geophys. Res. https://doi.org/10.1029/2003JD004473.

Philipp, A., Bartholy, J., Beck, C., Erpicum, M., Esteban, P., Fettweis, X., Huth, R., James, P., Jourdain, S., Kreienkamp, F., Krennert, T., Lykoudis, S., Michalides, S.C., Pianko-Kluczynska, K., Post, P., Alvarez, D.R., Schiemann, R., Spekat, A., Tymvios, F. S., 2010. Cost733cat - a database of weather and circulation type classifications. Phys. Chem. Earth 35, 360–373. https://doi.org/10.1016/j.pce.2009.12.010.

Price, C., Rind, D., 1992. A simple lightning parameterization for calculating global lightning distributions. J. Geophys. Res. 97 https://doi.org/10.1029/92JD00719.

Qu, Z., Henze, D.K., Cooper, O.R., Neu, J.L., 2020. Impacts of global NO_x inversions on NO_2 and ozone simulations. Atmos. Chem. Phys. 20, 13109–13130. https://doi.org/10.5194/acp-20-13109-2020.

Shu, L., Xie, M., Wang, T., Gao, D., Chen, P., Han, Y., Li, S., Zhuang, B., Li, M., 2016. Integrated studies of a regional ozone pollution synthetically affected by subtropical high and typhoon system in the Yangtze River Delta region, China. Atmos. Chem. Phys. 16 (24), 15801–15819. https://doi.org/10.5194/acp-16-15801-2016.

Travis, K., Jacob, D., 2019. Systematic bias in evaluating chemical transport models with maximum daily 8-hour average (MDA8) surface ozone for air quality applications. Geosci. Model Dev. Discuss. 1-13 https://doi.org/10.5194/gmd-2019-78.

Wang, Y., Jacob, D., Logan, J., 1998. Global simulation of tropospheric O_3 NO_x-hydrocarbon chemistry 3. Origin of tropospheric ozone and effects of nonmethane hydrocarbons. J. Geophys. Res. 103, 10757–10767. https://doi.org/10.1029/98JD00156.

Wang, X., Zhang, Y., Hu, Y., Zhou, W., Lu, K., Zhong, L., Zeng, L., Shao, M., Hu, M., Russell, A.G., 2010. Process analysis and sensitivity study of regional ozone formation over the Pearl River Delta, China, during the PRIDE-PRD2004 campaign using the Community Multiscale Air Quality modeling system. Atmos. Chem. Phys. 10 (9), 4423–4437. https://doi.org/10.5194/acp-10-4423-2010.

Wang, P., Chen, Y., Hu, J., Zhang, H., Ying, Q., 2019a. Source apportionment of summertime ozone in China using a source-oriented chemical transport model. Atmos. Environ. 211, 79–90. https://doi.org/10.1016/j.atmosenv.2019.05.006.

Wang, N., Lyu, X., Deng, X., Huang, X., Jiang, F., Ding, A., 2019b. Aggravating O_3 pollution due to NO_x emission control in eastern China. Sci. Total Environ. 677, 732–744. https://doi.org/10.1016/j.scitotenv.2019.04.388.

Wang, M., Yim, S., Wong, D., Ho, K., 2019c. Source contributions of surface ozone in China using an adjoint sensitivity analysis. Sci. Total Environ. 662, 385–392. https://doi.org/10.1016/j.scitotenv.2019.01.116.

Wang, Y., Wang, J., Xu, X., Henze, D.K., Qu, Z., Yang, K., 2020. Inverse modeling of SO_2 and NO_x emissions over China using multisensor satellite data – part 1: formulation and sensitivity analysis. Atmos. Chem. Phys. 20, 6631–6650. https://doi.org/10.5194/acp-20-6631-2020.

Wang, W., van der A, R., Ding, J., van Weele, M., Cheng, T., 2021a. Spatial and temporal changes of the ozone sensitivity in China based on satellite and ground-based observations. Atmos. Chem. Phys. 21 (9), 7253–7269. https://doi.org/10.5194/acp-21-7253-2021.

Wang, Xiaolin, Fu, T.M., Zhang, L., Cao, H., Zhang, Q., Ma, H., Shen, L., Evans, M.J., Ivatt, P.D., Lu, X., Chen, Y., Zhang, L., Feng, X., Yang, X., Zhu, L., Henze, D.K., 2021b. Sensitivities of ozone air pollution in the Beijing-Tianjin-Hebei area to local and upwind precursor emissions using adjoint modeling. Environ. Sci. Technol. 55 (9), 5752–5762. https://doi.org/10.1021/acs.est.1c00131.

Wang, Xinqi, Xiang, Y., Liu, W., Lv, L., Dong, Y., Fan, G., Ou, J., Zhang, T., 2021c. Vertical profiles and regional transport of ozone and aerosols in the Yangtze River Delta during the 2016 G20 summit based on multiple lidars. Atmos. Environ. 259 https://doi.org/10.1016/j.atmosenv.2021.118506.

Wang, W., Parrish, D.D., Wang, S., Bao, F., Ni, R., Li, X., Yang, S., Wang, H., Cheng, Y., Su, H., 2022a. Long-term trend of ozone pollution in China during 2014–2020: distinct seasonal and spatial characteristics and ozone sensitivity. Atmos. Chem. Phys. 22 (13), 8935–8949. https://doi.org/10.5194/acp-22-8935-2022.

Wang, T., Xue, L., Feng, Z., Dai, J., Zhang, Y., Tan, Y., 2022b. Ground-level ozone pollution in China: a synthesis of recent findings on influencing factors and impacts. Environ. Res. Lett. 17 (6) https://doi.org/10.1088/1748-9326/ac69fe.

Werf, G., Randerson, J., Giglio, L., Leeuwen, T., Chen, Y., Rogers, B., Mu, M., Marle, M. V., Morton, D., Collatz, G., Yokelson, R., Kasibhatla, P., 2017. Global fire emissions estimates during 1997–2016. Earth Syst. Sci. Data 9, 697–720. https://doi.org/10.5194/essd-9-697-2017.

Xian, M., Liu, X., Song, K., Gao, T., 2020. Reconstruction and nowcasting of rainfall field by oblique earth-space links network: preliminary results from numerical simulation. Remote Sens. 12 (21) https://doi.org/10.3390/rs12213598.

Xiao, Z., Miao, Y., Du, X., Tang, W., Yu, Y., Zhang, X., Che, H., 2020. Impacts of regional transport and boundary layer structure on the PM2.5 pollution in Wuhan, Central China. Atmos. Environ. 230 https://doi.org/10.1016/j.atmosenv.2020.117508.

Xu, Z., Huang, X., Nie, W., Shen, Y., Zheng, L., Xie, Y., Wang, T., Ding, K., Liu, L., Zhou, D., Qi, X., Ding, A., 2018. Impact of biomass burning and vertical mixing of residual-layer aged plumes on ozone in the Yangtze River Delta, China: a tethered-balloon measurement and modeling study of a multiday ozone episode. J. Geophys. Res. Atmos. 123 (20), 11,786–11,803. https://doi.org/10.1029/2018jd028994.

Yang, Y., Zhao, Y., Zhang, L., Zhang, J., Huang, X., Zhao, X., Zhang, Y., Xi, M., Lu, Y., 2021. Improvement of the satellite-derived NO_x emissions on air quality modeling and its effect on ozone and secondary inorganic aerosol formation in the Yangtze River Delta, China. Atmos. Chem. Phys. 21 (2), 1191–1209. https://doi.org/10.5194/acp-21-1191-2021.

Ye, X., Song, Y., Cai, X., Zhang, H., 2016. Study on the synoptic flow patterns and boundary layer process of the severe haze events over the North China Plain in January 2013. Atmos. Environ. 124, 129–145. https://doi.org/10.1016/j.atmosenv.2015.06.011.

Zhang, L., Jacob, D.J., Kopacz, M., Henze, D.K., Singh, K., Jaffe, D.A., 2009. Intercontinental source attribution of ozone pollution at western U.S. sites using an adjoint method. Geophys. Res. Lett. 36 (11) https://doi.org/10.1029/2009gl037950.

Zhang, K., Huang, L., Li, Q., Huo, J., Duan, Y., Wang, Y., Yaluk, E., Wang, Y., Fu, Q., Li, L., 2021. Explicit modeling of isoprene chemical processing in polluted air masses in suburban areas of the Yangtze River Delta region: radical cycling and formation of ozone and formaldehyde. Atmos. Chem. Phys. 21 (8), 5905–5917. https://doi.org/10.5194/acp-21-5905-2021.

Zhao, Z., Zhou, Z., Russo, A., Du, H., Xiang, J., Zhang, J., Zhou, C., 2021. Impact of meteorological conditions at multiple scales on ozone concentration in the Yangtze River Delta. Environ. Sci. Pollut. Res. Int. 28 (44), 62991–63007. https://doi.org/10.1007/s11356-021-15160-2.

Zheng, B., Tong, D., Li, M., Liu, F., Hong, C., Geng, G., Li, H., Li, X., Peng, L., Qi, J., Yan, L., Zhang, Y., Zhao, H., Zheng, Y., He, H., Zhang, Q., 2018. Trends in China's anthropogenic emissions since 2010 as the consequence of clean air actions. Atmos. Chem. Phys. 18, 14095–14111. https://doi.org/10.5194/acp-18-14095-2018.

Zong, L., Yang, Y., Xia, H., Yuan, J., Guo, M., 2023. Elucidating the impacts of various atmospheric ventilation conditions on local and transboundary ozone pollution patterns: a case study of Beijing, China. J. Geophys. Res. Atmos. 128 (20) https://doi.org/10.1029/2023jd039141.